SPECTROSCOPIC STUDY OF THE N159/N160 COMPLEX IN THE LARGE MAGELLANIC CLOUD

CECILIA FARIÑA[1,2], GUILLERMO L. BOSCH[1,2], NIDIA I. MORRELL[3], RODOLFO H. BARBÁ[4,5], AND NOLAN R. WALBORN[6]

[1] Facultad de Ciencias Astronómicas y Geofísicas, Universidad Nacional de La Plata, 1900 La Plata, Argentina; ceciliaf@fcaglp.unlp.edu.ar
[2] IALP-CONICET, Argentina
[3] Las Campanas Observatory, Observatories of the Carnegie Institution of Washington, La Serena, Chile
[4] Complejo Astronómico El Leoncito, Avda. España 1412 Sur, San Juan, Argentina
[5] Departamento de Física, Universidad de La Serena, Benavente 980, La Serena, Chile
[6] Space Telescope Science Institute, 3700 San Martin Drive, Baltimore, MD 21218, USA

ABSTRACT

We present a spectroscopic study of the N159/N160 massive star-forming region south of 30 Doradus in the Large Magellanic Cloud, classifying a total of 189 stars in the field of the complex. Most of them belong to O and early B spectral classes; we have also found some uncommon and very interesting spectra, including members of the Onfp class, a Be P Cygni star, and some possible multiple systems. Using spectral types as broad indicators of evolutionary stages, we considered the evolutionary status of the region as a whole. We infer that massive stars at different evolutionary stages are present throughout the region, favoring the idea of a common time for the origin of recent star formation in the N159/N160 complex as a whole, while sequential star formation at different rates is probably present in several subregions.

Key words: galaxies: starburst – H II regions – ISM: individual: (N159/N160) – Magellanic Clouds – stars: early type

Online-only material: color figure, figure set, extended figure

1. INTRODUCTION

The N159/N160 complex comprises a star-forming region located in the Large Magellanic Cloud (LMC), approximately 600 pc in projection south of 30 Doradus. The complex extension, from north to south, is approximately 15′ (225 pc) (Nakajima et al. 2005). Several reasons motivate the present study of the N159/N160 complex. The most important to mention are the following.

1. The whole complex is populated by young massive stars and it presents numerous features characteristic of active star formation.
2. Its distance (approximately 50 kpc for the LMC) is small enough to permit study of individual objects (small scale), but also large enough to allow a broad view of the distribution of stars and interstellar matter over the whole complex (large scale).
3. There has been little spectral classification study of stars within the complex. Aside from a few conspicuous objects, spectral classes of individual stars have been inferred only from photometry or indirectly from UV photon fluxes.

The whole complex has been widely observed and studied at different frequencies. The H II regions in N159/N160 were first cataloged by Henize (1956). Gatley et al. (1981) discovered the first extragalactic protostar in this complex, and the same year, Caswell & Haynes (1981) found the first Type I extragalactic OH maser. Yamaguchi et al. (2001) performed a global study of CO in the LMC, focused on giant molecular clouds and their association with young objects, and they found a compact group of the youngest clusters ($t \leqslant 10$ Myr) located near N159 while those with ages between 10 and 30 Myr extend to the northern part of the complex (between 30 Dor and N159). Candidate Herbig Ae/Be and OB stars were detected in N159/N160 by

Nakajima et al. (2005), who found indications of sequential cluster formation within the complex and, on a major scale, from N160 to N159S. These authors also suggest a scenario for sequential formation. There are numerous studies on subregions within the complex. Most of them focused on N159 or part of it, as did, for example, Deharveng et al. (1992) and Deharveng & Caplan (1992), who obtained *UBVRI*, Hα, Hβ, and [O III] photometry of N159A. Additional *JHK* stellar photometry is available from Meynadier et al. (2004) and Heydari-Malayeri & Testor (1982) observed at Hα, Hβ, and [O III]; *UBVI* stellar photometry of the whole region can be found in the Magellanic Clouds Photometric Survey by Zaritsky et al. (2004). Bolatto et al. (2000) studied the carbon in the gaseous phase of the whole complex; the authors described N159/N160 as composed of three distinct and well separated regions, aligned from north to south, N160 lies in the northern part, N159 is at the center, and N159S is in the southern part, and they support the idea that different stages of stellar formation are being observed in these regions, which would be currently active in N159, while not yet present in N159S. However, the stellar component of the region has been the subject of independent studies using various techniques and covering different subregions. This circumstance might be biasing the global interpretation of what is taking place in this vast star-forming region. We have therefore conducted spectroscopic observations and performed a preliminary analysis of stars in the N159/N160 complex as a contribution to a better understanding of the star-forming history of the region.

Section 2 contains a description of the observations, data processing, and reductions. In Section 3, we present the spectral classification as well as comments on some individual interesting spectra. Section 4 presents a brief discussion and interpretation of the data. An Appendix summarizes the most important classification criteria and the meaning of special characters used in some spectral types.

2. OBSERVATIONS, DATA PROCESSING, AND REDUCTIONS

2.1. Spectroscopic Observations

The images were taken during two consecutive nights in 2003 November, at the Las Campanas Observatory (LCO), Chile, with the 2.5 m Irénée du Pont telescope and the Wide Field Reimaging CCD Camera, in the multi-object spectroscopic mode. The detector was a Tek#5 CCD with 2048×2048 (24 μm) pixels providing images of 25 arcmin diameter at a scale of 32.3 arcsec mm^{-1} (0.774 arcsec pixel^{-1}). The H&K grism, centered at 3700 Å, was used resulting in spectrograms with reciprocal dispersion of 1.3 Å pixel^{-1} and $\sim$3.1 Å resolution. We used nine different slit masks grouping stars of similar brightness, selected in order to produce the minimum overlapping among the resulting spectra. Each mask has an average of 25 slits of variable length and 1 arcsec wide. The number of spectra obtained in each mask depends on the number of stars falling in each slit. Individual exposures were 1200 s long; two or three exposures were taken for each slit mask to combine into the final spectra.

2.2. Source Selection

No optical photometry was available at the time the multislit masks were made, therefore program stars were selected from colors calculated from their Two Micron All Sky Survey (2MASS) *JHK* photometry. We derived an IR analogue to the Q parameter; $Q_{\mathrm{IR}} = (J - H) - (H - K)E_{J-H}/E_{H-K}$. Although we were aware that infrared photometry is even less sensitive than UBV for early-type stars, this parameter has behaved well in detecting OB stars in the area. Astrometry was derived using a set of stars common to our acquisition images and the 2MASS catalog.

2.3. Data Processing and Reductions

The data were reduced using the IRAF[7] software package at the La Plata Observatory. The bias level was removed but the images were not divided out by flat fields because the quartz lamp exposures were obtained with the multislit masks in and adjacent spectra slightly overlap each other. The subtraction of background nebular emission was not trivial in some of the spectra. Two situations are worth mentioning to illustrate this point.

1. In our multi-object spectroscopy masks several stars did not fall in the center of the slit, but rather near one of the ends, making it difficult to take a background sample large enough to be properly removed. This results in background contamination that is not easy to remove due to the fact that the nebular background emission in which the program stars are immersed is bright and highly variable on small spatial scales. Many of these are stars that were not originally included in the program but showed up as bonus spectra in program star slits.
2. Because the spectra are slightly curved along the dispersion direction, some spectra from consecutive slits are overlapped. This contamination from other slits prevented us from obtaining a proper sample of adjacent background emission.
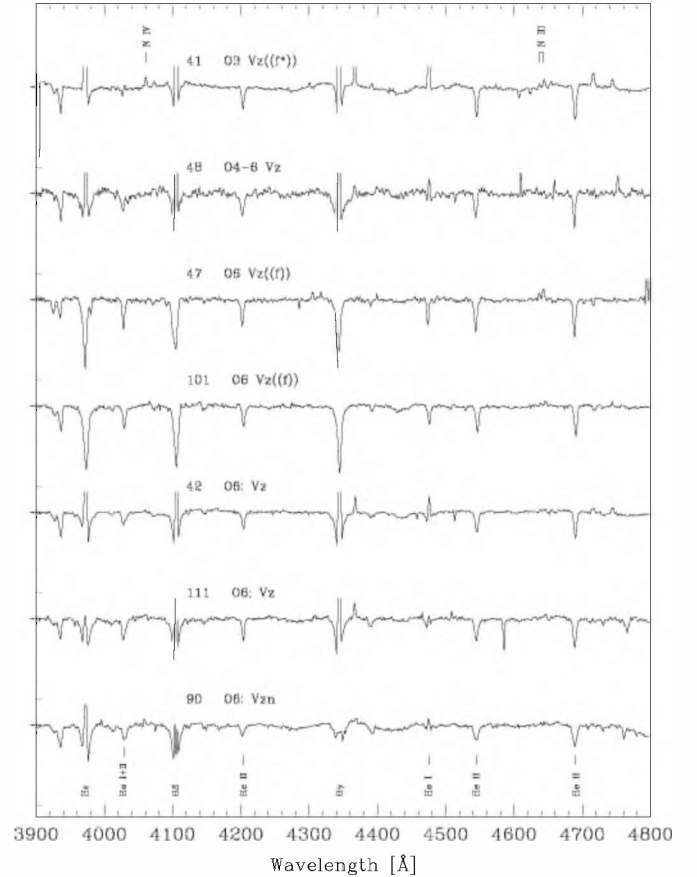

Figure 1. Normalized spectrograms of stars classified as early O-type dwarfs. Wavelength in Å is given on the *x*-axis, and on the *y*-axis thick long ticks mark the continuum flux while thin shorter ticks show the 0.8 continuum flux unit level. The spectral absorption features identified as reference are, from left to right by ion, He I+II λ4026, He II $\lambda\lambda$4200, 4541, 4686, and He I $\lambda\lambda$4471 absorption. Emission lines N IV λ4058 and N III $\lambda\lambda$4634-40-42 are also identified above star 41. Three Balmer series lines are also identified: Hϵ λ3970, Hδ λ4101, and Hγ λ4340.

(The complete Figure set (20 images) is available in the online journal.)

These are the reasons that in some of the spectra presented the background nebular emission is noticeable, although in most cases it does not affect the spectral classification. The signal-to-noise ratio (S/N) covers a range from 20 for the noisier spectra to 210 for those of best quality. The histogram distribution among these values is nearly flat.

3. RESULTS

3.1. Spectral Classification

The spectra were classified mainly following the criteria of the Digital Atlas of Optical Spectral Classification of OB Stars (Walborn & Fitzpatrick 1990). Other sources were consulted for some particular spectra, among them are the Digital Atlas of Peculiar Spectra (Walborn & Fitzpatrick 2000), The Spectral Classification System for the Earliest O Stars (Walborn et al. 2002) and R. O. Gray's Digital Atlas of Spectral Classification.[8] In Figure Set 1, the best quality spectra from our data set are presented, ordered by sequence of spectral type and luminosity class. In Table 1, all the stars for which we obtained a spectral classification are listed, along with their J2000 celestial

---

[8] http://nedwww.ipac.caltech.edu/level5/Gray/frames.html

Table 1
Spectral Classification of 189 Stars

Table 1
(Continued)

ID	α (J2000)	δ (J2000)	Spectral Type	V	ID	α (J2000)	δ (J2000)	Spectral Type	V
1	5:37:40.96	−69:48:32.9	O9	⋯	67	5:39:58.93	−69:39:25.4	O7 Vn	13.9
2	5:37:44.94	−69:41:59.1	A0 V	14.1	68	5:39:58.95	−69:43:51.8	O7 Vz	15.2
3	5:37:57.45	−69:38:16.0	A5 V	19.1	69	5:39:59.28	−69:43:57.7	O9.5 IV−III	14.5
4	5:37:59.60	−69:41:13.0	B2.5 V	17.2	70 #	5:39:59.29	−69:40:19.3	O9 Vn SB2 ?	14.7
5	5:38:14.05	−69:38:18.1	B1 − 3 V	19.2	71	5:39:59.30	−69:40:53.3	O9.5 V	15.5
6	5:38:20.28	−69:44:40.6	F0 Ib	16.4	72 #	5:39:59.81	−69:36:10.6	O6n(f+)p	13.7
7	5:38:26.73	−69:45:52.3	A0 Ib	10.9	73	5:40:00.28	−69:40:21.7	O6: III:	13.2
8	5:38:32.13	−69:37:10.4	G5 V	15.6	74	5:40:00.50	−69:42:14.6	F0 Ia	14.3
9	5:38:32.26	−69:35:41.5	B0 − 2 V	18.3	75	5:40:00.88	−69:41:09.8	O9 V	15.1
10	5:38:41.65	−69:35:44.1	A3 III	15.6	76 #	5:40:01.05	−69:34:52.8	A I + B ?	12.7
11	5:38:42.97	−69:35:42.8	A5 III	16.2	77	5:40:01.1	−69:46:02.5	O7 f/(f)	14.0
12	5:38:50.23	−69:46:47.9	A3 III−II	14.4	78	5:40:02.38	−69:40:59.1	B3 − 5 III	16.8
13	5:38:55.01	−69:38:47.4	A0 III−Ib	14.2	79	5:40:03.06	−69:43:52.1	B8 − 9 V−III	17.2
14	5:38:57.31	−69:47:57.8	G0 − 3 V	15.7	80	5:40:03.23	−69:40:58.7	B3 − 5 V−III	17.1
15	5:39:02.25	−69:39:54.8	G0 V	13.3	81	5:40:04.07	−69:43:51.7	O7n	14.2
16	5:39:08.92	−69:42:52.4	B1 Vn[e]	15.0	82 #	5:40:04.62	−69:39:50.6	O5n(f+)p	12.4
17	5:39:11.86	−69:42:20.0	G0 V	15.0	83	5:40:04.68	−69:39:20.0	B1 − 1.5 V	16.9
18	5:39:17.72	−69:42:42.1	G0 − 3 V	16.6	84	5:40:04.85	−69:40:59.1	B1.5 − 2 II	14.5
19	5:39:18.93	−69:36:58.2	B0.7 Ib	14.2	85	5:40:05.54	−69:39:18.9	B1.5 II	14.9
20	5:39:19.68	−69:40:13.2	B1 − 2 V	17.3	86	5:40:05.59	−69:46:05.4	B0.5 − 1 III	15.1
21	5:39:25.74	−69:42:42.7	A0 V	17.7	87	5:40:06.83	−69:45:42.9	O7 V:	13.9
22	5:39:30.42	−69:36:37.5	G0 V	15.7	88	5:40:08.18	−69:39:17.2	O4 III(f)	13.6
23	5:39:30.69	−69:39:12.3	O8 Vz	14.5	89	5:40:09.07	−69:47:00.1	O9	15.9
24	5:39:32.37	−69:40:12.6	B2 − 3 V	16.7	90	5:40:08.83	−69:40:22.1	O6: Vzn	15.1
25	5:39:32.66	−69:39:18.2	O6.5 Vz	14.5	91	5:40:09.45	−69:40:18.0	O8 − 8.5 V	13.6
26	5:39:34.29	−69:42:50.5	O7 Vz	15.3	92	5:40:10.56	−69:40:17.8	B1 V	14.2
27	5:39:34.90	−69:39:22.7	O8.5 V((f))	14.6	93 #	5:40:12.80	−69:34:54.6	BN0 Iabp	12.5
28	5:39:35.61	−69:39:12.5	O8 − 8.5 V	14.7	94	5:40:13.43	−69:34:45.2	O9.7 Ib	12.8
29	5:39:36.21	−69:37:13.7	O9 − 9.5 III−II	15.8	95	5:40:13.48	−69:43:50.3	K5 V	14.5
30	5:39:36.51	−69:39:24.1	B0 V	15.1	96	5:40:14.04	−69:38:06.7	O9.5 V(n)	14.8
31	5:39:36.86	−69:39:20.6	B1 − 2 V	16.6	97	5:40:14.26	−69:42:59.3	B0.2 − 0.5 V	15.1
32	5:39:37.17	−69:43:45.4	B0 Ia	14.4	98	5:40:15.60	−69:36:57.5	O8 II((f))	13.9
33 #	5:39:38.48	−69:38:23.5	O9.7 Iabpe	14.0	99	5:40:17.45	−69:46:24.1	O6:	14.8
34	5:39:38.50	−69:36:52.3	G5 V	14.4	100	5:40:17.85	−69:38:02.4	G5 V	16.2
35 #	5:39:38.88	−69:44:35.6	O8(f)p	14.6	101	5:40:17.91	−69:37:06.8	O6 Vz((f)	14.2
36	5:39:40.04	−69:43:52.2	G8 V−III	13.9	102	5:40:18.32	−69:36:33.4	O8.5 − 9 III	13.9
37 #	5:39:40.09	−69:46:19.6	O8	13.0	103	5:40:18.36	−69:37:17.3	B2.5 V	15.4
38 #	5:39:40.09	−69:44:33.7	B3 I(a)	12.1	104	5:40:19.32	−69:37:07.0	O8.5 III-II((f))	13.8
39 #	5:39:40.80	−69:38:33.7	O9.7 Ia+pe	13.0	105	5:40:19.64	−69:40:07.5	O9.5 V	15.6
40	5:39:41.61	−69:44:20.8	O6.5 V	14.7	106	5:40:20.21	−69:40:31.8	O8 − 8.5 Vz	15.3
41 #	5:39:43.9	−69:38:42.9	O3 Vz((f*))	⋯	107 #	5:40:20.58	−69:39:01.0	O6 Vn SB2 ?	14.5
42	5:39:44.17	−69:38:40.9	O6: Vz	⋯	108	5:40:20.90	−69:40:19.1	B0 − 0.2 V	15.3
43	5:39:44.41	−69:38:40.0	O8 − 9 V	13.8	109	5:40:20.93	−69:37:18.6	B5 III−I	16.2
44	5:39:44.52	−69:39:12.0	B1 − 3 III	15.6	110	5:40:23.64	−69:37:43.4	B5 − 8 V−III	18.1
45	5:39:44.94	−69:39:00.8	O8 − 8.5 Vz	13.6	111	5:40:24.75	−69:40:13.2	O6: Vz	12.4
46	5:39:44.96	−69:44:21.0	B2 − 3 III	17.9	112 #	5:40:24.78	−69:37:44.0	B2 − 2.5 SB2 ?	15.3
47	5:39:46.12	−69:43:57.1	O6 Vz((f)	14.3	113	5:40:25.00	−69:41:59.0	B0.5 − 1 V	15.3
48	5:39:46.14	−69:38:52.9	O4 − 6 Vz	13.8	114	5:40:25.20	−69:34:57.5	O9.5 Ib	13.8
49	5:39:46.80	−69:39:12.5	O6 V	14.8	115	5:40:25.98	−69:35:12.3	B1 Ib	14.0
50	5:39:49.67	−69:49:19.8	B1 − 2:	16.5	116	5:40:26.18	−69:41:32.4	O6.5 Vz	15.0
51	5:39:50.07	−69:39:35.9	O9 V	14.8	117	5:40:28.03	−69:36:12.2	O6.5 Vz	14.3
52	5:39:50.25	−69:43:54.0	B1.5 − 2 V	15.2	118	5:40:28.19	−69:35:13.7	O6 − 7:	16.3
53	5:39:50.40	−69:38:18.3	O6: V	15.3	119	5:40:28.38	−69:43:37.6	O8 − 9 V	14.9
54 #	5:39:51.13	−69:44:22.2	O4 − 6 Vn SB2 ?	14.4	120	5:40:29.68	−69:45:16.7	B0 V	15.9
55	5:39:52.47	−69:40:38.9	B0.5 − 1 V	14.4	121	5:40:30.46	−69:37:02.3	B1 − 1.5 III−II	15.1
56	5:39:52.69	−69:44:05.4	O9.5 V−III	15.8	122	5:40:31.32	−69:35:02.8	B2 V	15.6
57	5:39:52.74	−69:45:46.8	O8	14.4	123	5:40:33.42	−69:35:04.8	B1 − 1.5 III−II	14.3
58	5:39:54.30	−69:39:33.9	O7.5−III((f))	14.4	124	5:40:34.77	−69:39:40.3	B4 III−I	13.1
59	5:39:55.00	−69:44:25.8	O6 III(f)	14.3	125	5:40:35.53	−69:36:10.4	B5 V	18.1
60	5:39:55.89	−69:39:14.9	B1 V	16.4	126	5:40:37.28	−69:35:23.0	B0.7 Ib	13.8
61	5:39:56.41	−69:38:59.6	O9 − 9.5 V	15.1	127	5:40:38.58	−69:34:25.4	B2 V	15.1
62	5:39:57.09	−69:43:53.3	B1 − 2 IV−II	17.8	128	5:40:39.62	−69:44:32.2	K0 V	15.4
63	5:39:57.35	−69:38:59.4	O9 V	15.5	129	5:40:40.30	−69:36:42.9	B0 − 1 V	15.6
64	5:39:57.63	−69:39:14.8	B1 V	15.3	130	5:40:41.56	−69:37:33.0	O8 Vz	14.6
65	5:39:57.94	−69:46:03.2	B2 V	16.5	131	5:40:41.97	−69:45:12.4	F3 V	13.3
66	5:39:58.74	−69:44:04.1	O8.5 II((f))	12.5	132	5:40:44.96	−69:38:42.3	F7 V	12.8

Table 1
(Continued)

ID	α (J2000)	δ (J2000)	Spectral Type	V
133	5:40:48.14	−69:43:17.6	O6 V	15.2
134	5:40:48.33	−69:39:46.8	B1 III	15.0
135	5:40:48.45	−69:49:38.6	B	14.1
136	5:40:49.51	−69:42:41.9	B2 II	14.6
137	5:40:50.26	−69:38:41.8	B2 V	14.8
138	5:40:52.82	−69:40:14.0	B2 V	17.0
139	5:40:53.57	−69:43:04.9	G8 V	14.0
140	5:40:53.69	−69:40:16.9	B0.2 − 0.5 V	15.2
141	5:40:53.72	−69:40:13.1	B0.2 − 0.5 V	15.6
142	5:40:53.72	−69:47:43.2	G0 V	14.8
143	5:40:54.86	−69:40:37.5	B1 − 1.5 V	14.6
144	5:40:55.09	−69:42:39.4	A0 III−Ib	14.6
145	5:40:55.77	−69:39:13.5	O8.5 Ib(f)	14.6
146	5:40:58.02	−69:48:31.2	B0 − 0.2 V−IV	14.3
147	5:40:59.75	−69:38:40.0	BC1.5 Iab	12.2
148	5:41:01.21	−69:37:36.8	B1 V	15.1
149	5:41:04.74	−69:37:48.6	B1 − 1.5 V	14.8
150	5:41:06.48	−69:40:21.6	B1.5 Iab	13.5
151 #	5:41:09.77	−69:39:15.8	O7n(f)p	13.2
152	5:41:11.29	−69:44:31.1	O9 III	13.9
153	5:41:15.07	−69:36:17.0	B2 V	15.9
154	5:41:16.18	−69:32:31.9	B7 − 8 V	17.6
155	5:41:16.62	−69:36:18.1	B1 V	17.1
156	5:41:17.12	−69:32:33.1	B0.5 − 1 V	14.8
157	5:41:20.02	−69:42:50.5	F0 V	12.9
158	5:41:20.04	−69:36:22.4	B4 III−I	11.8
159	5:41:20.24	−69:35:59.8	B1 V	14.8
160	5:41:21.40	−69:38:49.4	O9.5 III	14.5
161	5:41:22.86	−69:47:19.4	G0 V	16.3
162	5:41:26.93	−69:36:11.4	B1 − 2 III−I	13.1
163	5:41:27.65	−69:48:03.0	B2.5: Ia:	17.2
164	5:41:27.86	−69:36:08.4	B2 V	16.0
165	5:41:28.05	−69:38:06.4	B1.5 − 2 III−II	12.8
166	5:41:29.43	−69:46:21.8	O9.7 II−Ib	12.3
167	5:41:30.44	−69:36:18.7	B1 II	14.0
168	5:41:30.66	−69:40:07.4	O9.7 Iab	12.6
169	5:41:30.97	−69:39:59.7	B1 IV	16.2
170	5:41:32.68	−69:40:01.9	B1 III−II	13.7
171	5:41:33.22	−69:39:44.2	BC1 Ia	13.5
172	5:41:35.30	−69:40:19.9	B1 III−II	15.0
173	5:41:35.54	−69:35:57.7	B1 Ia	12.8
174	5:41:38.03	−69:36:16.4	B3 − 5 V−III	18.4
175	5:41:38.85	−69:40:07.4	B0.5 IV	15.2
176	5:41:39.22	−69:49:24.2	B2: III−II:	12.7
177	5:41:40.08	−69:39:50.8	B1.5 Ib	13.7
178	5:41:40.98	−69:39:50.8	O8.5 − 9 III	13.6
179 #	5:41:43.71	−69:37:37.4	B Iae P Cyg	14.1
180	5:41:44.00	−69:41:24.6	A III	18.3
181	5:41:45.07	−69:40:03.5	F0 V	14.4
182	5:41:58.26	−69:39:50.1	A0: V−III	18.1
183	5:41:59.32	−69:43:44.1	A5 II−Ib	12.3
184	5:41:59.76	−69:40:04.0	B1 − 2 V−IV	17.0
185	5:42:01.00	−69:39:48.5	F5−G0 V−I	19.1
186	5:42:04.36	−69:39:48.8	G8 V−III	17.4
187	5:42:05.65	−69:41:23.0	B2 − 3 III	17.2
188	5:42:05.95	−69:40:04.1	B1 − 2 V	17.6
189	5:42:10.13	−69:38:45.8	B3 − 5 V	17.3

Notes. Column 1 lists our internal nomenclature for the observed objects, objects are listed by R.A. Stars marked with "#" have individual comments in Section 3.2. Celestial coordinates (J2000), obtained through 2MASS astrometry, are shown in Columns 2 and 3. Spectral classification from our data is given in Column 4. Column 5 shows, as a reference, V magnitudes from the Zaritsky et al. (2004) photometric survey for all the objects, except for stars 1, 41, and 42 for which the catalog correlation was uncertain.

Table 2
Stars with Spectral Classification Found in the Literature

ID	Spectral Type (This Work)	Sanduleak (ID, Spectral Type)	Spectral Type (Other)
7	A0 Ib	Sk −69 242, A2 I	A7 (HD)
			A2 Ia0 (A−P)
			A0 Ia (S)
35	O8(f)p	···	LMC X-1 (HC)
			O7 − 9 III (MP-B)
37	O8	···	O3-O6 V (C)
38	B3 I(a)	Sk −69 254, OB	B3 I(Nstr)+neb (F)
			B5+neb (R−P)
66	O8.5 II((f))	Sk −69 257, OB	B0.5 (R−P)
			O9 II (W)
73	O6: III:	···	B1-2 (BI-263)
82	O5n(f+)p	···	OB0 (BI-265)
			O6 V(M)
147	BC1.5 Iab	Sk −69 268, OB	B2.5 (P)
150	B1.5 Iab	Sk −69 269, OB:	B1 III: (M)
158	B4 III−I	Sk −69 271, OB	B2 (P)
			HXMB (L)
163	B2.5: Ia:	Sk −69 274, OB:	B2 Ia (A−P−R)
			Con (HD)
			B2.5 Ia (F)
173	B1 Ia	Sk −69 275, OB	B1.5 (P)
176	B2: III−II:	Sk −69 277, OB	B1.5 (P)
183	A5 II−Ib	···	A5 (HD)
			A5 I (P)

Notes. Column 1 identifies stars according to Table 1. Column 2 repeats our spectral classification already given in Table 1, Column 3 contains spectral types from Sanduleak (1970), and Column 4 lists classification from other sources which are individually labeled.

References. (HD) Cannon & Pickering 1918; (BI) Brunet et al. 1975; (R) Feast et al. 1960; (C) Conti & Fitzpatrick 1991; (A) Ardeberg et al. 1972; (P) Rousseau et al. 1978; (F) Fitzpatrick 1991; (W) Walborn 1977; (L) Liu et al. 2000; (MP) Pakull 1984; (B) Bianchi & Pakull 1985; (HC) Hutchings et al. 1983; (M) Massey et al. 1995; (S) Stock et al. 1976.

coordinates and V magnitudes from Zaritsky et al. (2004). Correlation between our star list and the photometric catalog was made by coordinates and we exclude magnitudes for three stars that seem to be misidentified: star 1 is very close to the limit of our field image and stars 41 and 42 are very close together, immersed in a bright background. In Table 2, we have listed our program stars that had already been classified by other authors. As mentioned in the introduction, only a few of the stars in our sample have previous spectral classifications based on spectroscopic observations, although many of them are included in several studies, see Meynadier et al. (2004), Degioia-Eastwood et al. (1993), Heydari-Malayeri et al. (2002), and Jones et al. (2005) among others. As can be seen, only nine stars were included in Sanduleak (1970) and the spectral class given is no more precise than "OB" type, except for Star 7. A few stars were also found in common with other catalogs of spectral classification through careful review of finding charts, since the difference in accuracy between the 2MASS coordinates and those in old catalogs made it impossible to search objects by coordinates.

3.2. Comments on Individual Interesting Spectra

Star 33 (Figure 1.8) has a peculiar spectrum, which was classified as O9.7 Iabpe. It presents emission at Hγ and all the lines appear peculiarly weak for a supergiant star.

Star 35 (Figure 1.9) is a widely studied object because it is the optical counterpart to the X-ray source LMC X-1. Hutchings et al. (1983) found it to be an O7 star with a binary period of approximately 4 days; they also suggested that the secondary could be a black hole. It was later classified as O7-9 III by Pakull (1984) and Bianchi & Pakull (1985). We find a type of O8(f)p, where the peculiarity refers to the reversed He II λ4686 emission. For this reason it has been associated with the Onfp class by N. R. Walborn et al. (2009, in preparation), of which the He II profile is a defining characteristic, although in this object the absorption lines are not broadened, and the He II profile may be related to the X-ray binary system.

Star 37 (Figure 1.4) was classified as O8 here, although Conti & Fitzpatrick (1991) classified it as O3–O6, based on the presence of He II λλ4200, 4541, 4686 absorption lines and possible N III λλ4634-40-42 emission lines. The stellar He I absorption lines were obliterated by the very strong nebular emission lines in their observation. For our classification we used mainly the ratios of He II λ4541/He I λ4387 and He II λ4200/He I λ4144. We also used the oversubtracted nebular [O III] λ4363 line present in the final spectrum to estimate the nebular oversubtraction (see Bosch et al. 1999). We found a correction of less than 15%, which indicates that the stellar He I λ4471 absorption is indeed deeper than He II λ4541. In addition, the C III λ4070 absorption blend is present. All of these considerations indicate that the spectral type of Star 37 must be closer to O8. Unfortunately, our wavelength coverage for this object did not allow us to check for the presence of N III emission, as suspected by Conti & Fitzpatrick (1991). The luminosity class could not be assessed due to the lack of the He II λ4686 line.

Star 38 (Figure 1.17) is a B3 supergiant that at one time was also a candidate for identification with LMC X-1. Fortunately, the weak He II λ4686 emission seen in high S/N digital data was not visible in the early observations, or this misidentification would have been considered definite! Ramsey et al. (2006) have clearly shown that this anomalous emission feature actually arises in an unusual high-ionization nebulosity in the field, which may be related to the X-ray source.

Star 39 (Figure 1.8) was classified as O9.7 Ia+pe. It is certainly an unusual spectrum, probably related to the Ofpe/WN9 or WNL class. See, for comparison, the spectrum of HD 152408 (Walborn et al. 2000). However, these characteristics have not been seen before at such a late O type.

Star 41 (Figure 1.1) is the hottest star we have found among the sample. It was classified as O3 Vz((f*)), although the z nature (He II λ4686 absorption stronger than other He lines, possibly an indicator of subluminosity and extreme youth) is marginal. N III λλ4634-40-42 and N IV λ4058 are clearly detected in emission and N V λλ4604-20 absorption lines are also present. Si IV λλ4089-4116 seem to be in emission but the features are not conspicuous.

Star 93 (Figure 1.10) was classified as BN0 Iabp due to enhanced N III and deficient C and O lines, characteristic of OBN stars (Walborn 1971a, 1976). The additional peculiarity is the presence of P Cygni profiles at Hγ and He I lines.

Star 179 (Figure 1.10) was classified as B Iae P Cyg. The P Cygni features can be seen in Hε and Hδ, but not in Hγ which is totally in emission. This object is quite similar to HD 87643 (Walborn & Fitzpatrick 2000), which belongs to the group of Iron Stars, of which η Carinae is the most famous member.

Stars 54, 70, 76, 107, and 112 (Figure 1.20) show either anomalously broad or asymmetric profiles in their absorption lines, suggesting a possible binary nature. The wavelength resolution does not allow us to reliably analyze radial velocity information. Higher resolution spectra would be needed to assess the possibility of these being SB2 stars.

Stars 72, 82, and 151 (Figure 1.9) belong to the Onfp category (Walborn 1973). In their spectra, the broad emission in He II λ4686 with absorption reversal can be observed (see the Appendix). Stars 72 and 82 are also denoted with "+" due to Si IV λ4116 emission; they also present C III λ4650 in emission. A luminosity class cannot be inferred for these stars because of the peculiar He II λ4686 profiles (N. R. Walborn et al. 2009, in preparation).

3.3. Discussion

30 Doradus is the current optical "hot spot" near the northeastern edge of a much larger, oval region several kpc in diameter, itself northeast of the LMC Bar, in which star formation has been active for at least 10^8 yr. This region contains half the WR content of the LMC, numerous young clusters of various ages, many red supergiants, and SN 1987A. The field south of 30 Dor is particularly rich in clusters, associations, and nebulae, including the N159/N160 complex studied here. This field also contains the most massive CO concentrations in the LMC, so it may be expected that in a few million years 30 Dor's successor will appear there. In order to analyze the current, global evolutionary trends within the N159/N160 complex, the observed stars have been grouped following qualitative criteria based on those defined and used in Walborn & Blades (1997); see also Bosch et al. (1999). We have defined three groups of spectral types and luminosity classes. These groups comprise distinct age ranges in massive stellar evolution. Then from the total of 189 spectra in the field of N159/N160, we have selected those that belong to one of the following three groups.

1. Young phase: O3-5 V-I and O Vz.
2. Middle-age phase: O6-9 V-I and B0 I.
3. Evolved phase: B0-2 V-III and B1-8 I.

Of course, some of the main-sequence stars in the second and third groups could actually belong to the younger ones, but this grouping is a first approximation for our purposes. The three groups are plotted in a direct image of the field in Figure 2, with different symbols for each. If a global sequential star formation process were taking place (as suggested by CO studies mentioned in Section 1 and also studies of neighboring regions like N158 (Testor & Niemela 1998)), we would expect to find systematic trends in the object distribution according to their evolutionary stages. Indeed, there is evidence for such effects in Figure 2.1: there is a clear tendency for the two younger phases to be associated with the nebulae and clusters, while the majority of the third phase are in the dispersed northeast quadrant of the field, which is devoid of nebulosity. On the other hand, young phase objects are found in the northern part of the complex (N160) as well as in the southern part (N159), while some more evolved objects also appear in the latter. Of course, we are looking at a two-dimensional projection of three-dimensional structures. It is quite likely that the younger concentrations are embedded in and/or projected against a field of more evolved and dispersed objects, just as occurs in 30 Dor itself (Walborn & Blades 1997; Selman et al. 1999). Also, some isolated very young objects may be runaways from the young clusters. Our data favor a scenario in which star formation was initiated throughout the region, perhaps in the event producing the kpc-scale structure noted above, and that
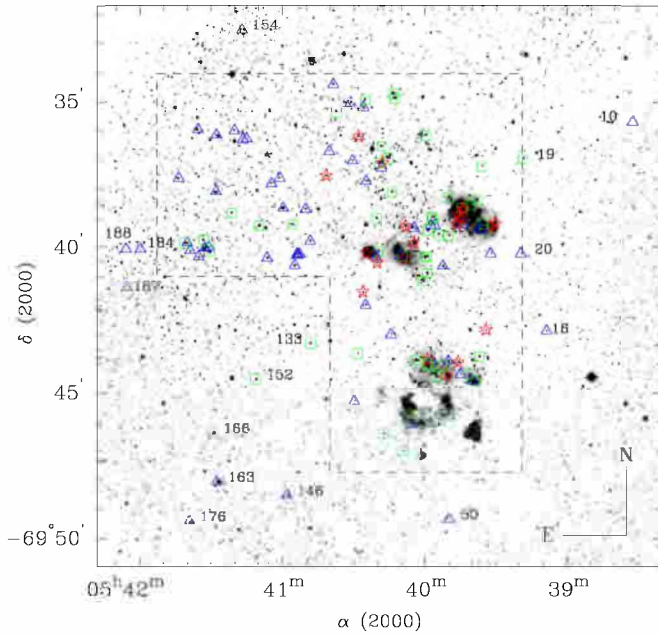
Figure 2. Spatial distribution of the stars on the sky distinguished by their spectral types, as an approximate indication of their evolutionary stages. The symbols are as follows: red stars, O3-O5 V-I and O Vz; green squares, O6-O9 V-I and B0 I; blue triangles, B0-B2 V-III and B1-B8 I. The dashed lines contour the regions that are zoomed in the online version of the figure. Stars outside the contours are labeled with their ID numbers from Table 1. Stars inside the contours are identified in the corresponding figure of the online version.

(An extended color version of this figure is available in the online journal.)

this strong burst led to subsequent, localized star formation events wherever sufficient remanent molecular material was available, in an ongoing process that continues at the present time. This scenario is in good agreement with other studies of subregions in the N159/N160 complex, as in Heydari-Malayeri et al. (2002) where the presence of compact high-excitation H II blobs demonstrates that this is indeed a very young subregion likely containing different (early) evolutionary stages. Stellar spectra alone do not provide the definitive ages that are required to construct a quantitative star formation history of the region. A complete photometric study will be essential to disentangle the overlapping populations and their extinctions. Such data are available from Zaritsky et al. (2004) and will be extended by new observations we are currently undertaking. Subsequently, we shall undertake a more detailed analysis including H–R diagrams and comparison with the extensive Hα, IR, and CO observations available for this region.

APPENDIX

CLASSIFICATION CRITERIA FOR OB STARS

General remarks. For spectral types from O3 to B0 V, the principal horizontal (spectral type or temperature) classification criteria are He II λ4541/He I λ4471 and He II λ4200/He I (+He II) λ4026. At the later types He II λ4541/He I λ4387 and He II λ4200/He I λ4144 are useful checks, since the former ratios become very small (but the latter ratios are also sensitive to luminosity).

For early B type spectra, the principal horizontal classification criterion shifts from the He ionization ratio to those of Si, first Si III λ4552/Si IV λ4089 and then Si II λλ4128-4130/Si III λ 4552.

In O-type spectra (earlier than O9), luminosity class V is defined by He II λ4686 strongly in absorption, class III by weakened absorption in that line, class Ib by an absent or neutralized line (filled in by emission), and Ia (or just I at the earliest types) by this line in emission above the continuum. Note that there are differences of detail in this sequence as a function of the spectral type; the two-dimensional types are ultimately defined by the standards. The designation Vz corresponds to spectra with He II λ4686 absorption stronger than any other He lines, possibly indicating subluminosity and extreme youth (on or near the Zero-Age Main-Sequence).

Concerning the different flavors of "f" effects. Of supergiants: strong He II λ4686 and N III λλ4634,4640-42 emission lines (Walborn 1971b). f+ denotes spectra in which Si IV λλ4089,4116 are present in emission (sometimes only the latter is visible due to cancellation of absorption and emission in the former). This category does not include objects in which the intense lines are of P Cygni type (Walborn & Fitzpatrick 2000). f* means that N IV λ4058 emission is stronger than N III λ4640, and is characteristic of O2–O3 spectra (Walborn & Fitzpatrick 1990; Walborn et al. 2002). Onfp Stars are characterized by broad, centrally reversed He II λ4686 emission, together with broadened absorption lines. There is a range in profiles from strong absorption with very weak emission wings to strong emission "split" by a weak absorption feature. In some cases, the two emission wings are unequal in intensity. These effects may be related to rapid rotation and/or a disk structure. Only a few of these objects are known and most of them are found in the Magellanic Clouds (Walborn 1973; Walborn et al. 2009, in preparation). In main-sequence stars (luminosity class V), ((f)) is used to denote strong He II λ4686 absorption accompanied by weak N III λλ4634,4640-42 emission. In the intermediate luminosity classes, (f) is used when the He II λ4686 absorption weakens and may become neutralized by emission, while the N III emission strength increases. Finally, Of supergiants have both He II and N III strongly in emission (Walborn & Fitzpatrick 1990).

Additional notes. The "n" parameter describes the degree of broadening of the spectral lines. The symbol ((n)) indicates that the lines of Si IV λ4116 and He I λ4121 are just merged (at ∼ 1 Å resolution), and (n) represents an intermediate case between that and the broadening in the n spectra. High rotational velocities are associated with this behavior (Walborn 1971b). A ":" after the spectral type or luminosity class denotes, as usual, that an accurate classification cannot be given due to one of several reasons, e.g., incomplete wavelength coverage, low S/N, uncertain continuum normalization.

In addition to the [O III] and H I lines, several He and Ne nebular lines are present in the observed spectra. Among

these, the He I $\lambda4471$ line is particularly important, as the corresponding stellar absorption line constitutes one of the principal horizontal classification criteria for O stars (He II $\lambda4541$/He I $\lambda4471$ ratio). Therefore, in some cases in which the nebular background emission could not be totally removed from the stellar spectra, a less accurate classification was achieved.

REFERENCES

Ardeberg, A., Brunet, J. P., Maurice, E., & Prevot, L. 1972, A&AS, 6, 249
Bianchi, L., & Pakull, M. 1985, A&A, 146, 242
Bolatto, A. D., Jackson, J. M., Israel, F. P., Zhang, X., & Kim, S. 2000, ApJ, 545, 234
Bonnarel, F., et al. 2000, A&AS, 143, 33
Bosch, G., Terlevich, R., Melnick, J., & Selman, F. 1999, A&AS, 137, 21
Brunet, J. P., Imbert, M., Martin, N., Mianes, P., Prévot, L., Rebeirot, E., & Rousseau, J. 1975, A&AS, 21, 109
Cannon, A. J., & Pickering, E. C. 1918, Annals of Harvard College Observatory, 92, 1
Caswell, J. L., & Haynes, R. F. 1981, MNRAS, 194, 33P
Conti, P. S., & Fitzpatrick, E. L. 1991, ApJ, 373, 100
Degioia-Eastwood, K., Meyers, R. P., & Jones, D. P. 1993, AJ, 106, 1005
Deharveng, L., & Caplan, J. 1992, A&A, 259, 480
Deharveng, L., Caplan, J., & Lombard, J. 1992, A&AS, 94, 359
Feast, M. W., Thackeray, A. D., & Wesselink, A. J. 1960, MNRAS, 121, 337
Fitzpatrick, E. L. 1991, PASP, 103, 1123
Gatley, I., Becklin, E. E., Hyland, A. R., & Jones, T. J. 1981, MNRAS, 197, 17P
Henize, K. G. 1956, ApJS, 2, 315
Heydari-Malayeri, M., Charmandaris, V., Deharveng, L., Meynadier, F., Rosa, M. R., Schaerer, D., & Zinnecker, H. 2002, A&A, 381, 941
Heydari-Malayeri, M., & Testor, G. 1982, A&A, 111, L11

Hutchings, J. B., Crampton, D., & Cowley, A. P. 1983, ApJ, 275, L43
Jones, T. J., Woodward, C. E., Boyer, M. L., Gehrz, R. D., & Polomski, E. 2005, ApJ, 620, 731
Liu, Q. Z., van Paradijs, J., & van den Heuvel, E. P. J. 2000, A&AS, 147, 25
Massey, P., Lang, C. C., Degioia-Eastwood, K., & Garmany, C. D. 1995, ApJ, 438, 188
Meynadier, F., Heydari-Malayeri, M., Deharveng, L., Charmandaris, V., Le Bertre, T., Rosa, M. R., Schaerer, D., & Zinnecker, H. 2004, A&A, 422, 129
Nakajima, Y., et al. 2005, AJ, 129, 776
Pakull, M. W. 1984, in IAU Symp. 108, Structure and Evolution of the Magellanic Clouds, ed. S. van den Bergh & K. S. D. Boer (Dordrecht: Kluwer), 317
Ramsey, C. J., Williams, R. M., Gruendl, R. A., Chen, C.-H. R., Chu, Y.-H., & Wang, Q. D. 2006, ApJ, 641, 241
Rousseau, J., Martin, N., Prévot, L., Rebeirot, E., Robin, A., & Brunet, J. P. 1978, A&AS, 31, 243
Sanduleak, N. 1970, Contributions from the Cerro Tololo Inter-American Observatory, 89
Selman, F., Melnick, J., Bosch, G., & Terlevich, R. 1999, A&A, 347, 532
Stock, J., Osborn, W., & Ibañez, M. 1976, A&AS, 24, 35
Testor, G., & Niemela, V. 1998, A&AS, 130, 527
Walborn, N. R. 1971a, ApJ, 164, L67
Walborn, N. R. 1971b, ApJS, 23, 257
Walborn, N. R. 1973, AJ, 78, 1067
Walborn, N. R. 1976, ApJ, 205, 419
Walborn, N. R. 1977, ApJ, 215, 53
Walborn, N. R., & Blades, J. C. 1997, ApJS, 112, 457
Walborn, N. R., & Fitzpatrick, E. L. 1990, PASP, 102, 379
Walborn, N. R., & Fitzpatrick, E. L. 2000, PASP, 112, 50
Walborn, N. R., Lennon, D. J., Heap, S. R., Lindler, D. J., Smith, L. J., Evans, C. J., & Parker, J. W. 2000, PASP, 112, 1243
Walborn, N. R., et al. 2002, AJ, 123, 2754
Yamaguchi, R., et al. 2001, PASJ, 53, 985
Zaritsky, D., Harris, J., Thompson, I. B., & Grebel, E. K. 2004, AJ, 128, 1606